A TLR4-derived non-cytotoxic, self-assembling peptide functions as a vaccine adjuvant in mice

Received for publication, March 7, 2018, and in revised form, September 1, 2018 Published, Papers in Press, November 1, 2018, DOI 10.1074/jbc.RA118.002768

Anshika Tandon[‡], Manisha Pathak[§], Munesh Kumar Harioudh[‡], Sabahuddin Ahmad[‡], Mohd Sayeed[‡], Tayyaba Afshan[‡], M. I. Siddiqi[‡], Kalyan Mitra[¶], Shailja M. Bhattacharya[§], and Jimut Kanti Ghosh[‡1]

From the [‡]Molecular and Structural Biology Division, [§]Division of Parasitology, and [¶]Electron Microscopy Unit, SAIF Division, CSIR-Central Drug Research Institute, Sector 10, Jankipuram Extension, Sitapur Road Lucknow–226 031, India

Edited by Luke O'Neill

Vaccination is devised/formulated to stimulate specific and prolonged immune responses for long-term protection against infection or disease. A vaccine component, namely adjuvant, enhances antigen recognition by the host immune system and thereby stimulates its cellular and adaptive responses. Especially synthetic Toll-like receptor (TLR) agonists having self-assembling properties are considered as good candidates for adjuvant development. Here, a human TLR4-derived 20-residue peptide (TR-433), present in the dimerization interface of the TLR4–myeloid differentiation protein-2 (MD2) complex, displayed self-assembly and adopted a nanostructure. Both *in vitro* studies and *in vivo* experiments in mice indicated that TR-433 is nontoxic. TR-433 induced pro-inflammatory responses in THP-1 monocytes and HEK293T cells that were transiently transfected with TLR4/CD14/MD2 and also in BALB/c mice. In light of the self-assembly and pro-inflammatory properties of TR-433, we immunized with a mixture of TR-433 and either ovalbumin or filarial antigen trehalose-6-phosphate phosphatase (TPP). A significant amount of IgG titers was produced, suggesting adjuvanting capability of TR-433 that was comparable with that of Freund's complete adjuvant (FCA) and appreciably higher than that of alum. We found that TR-433 preferentially activates type 1 helper T cell (T_h1) response rather than type 2 helper T cell (T_h2) response. To our knowledge, this is the first report on the identification of a short TLR4-derived peptide that possesses both self-assembling and pro-inflammatory properties and has significant efficacy as an adjuvant, capable of activating cellular responses in mice. These results indicate that TR-433 possesses significant potential for development as a new adjuvant in therapeutic application.

The purpose of vaccination is to stimulate effective and prolonged immune responses in a host against an antigen for long-term protection against an infection and/or disease. For successful accomplishment of vaccination, often an additional substance, namely adjuvant, is required that assists in the recognition of an antigen by the innate immune system, ultimately stimulating cellular and adaptive responses in the host (1–3). Over the decades, aluminum-based compounds (*e.g.* aluminum phosphate and hydroxide) remained the predominant human adjuvants. However, these aluminum salts are not perfect adjuvants because these are relatively weak with some of the antigens (*e.g.* malaria and tuberculosis) and they rarely induce cellular immune responses (4). Then Freund introduced the idea of co-delivery of inflammation-inducing agents like killed mycobacteria and developed Freund's complete adjuvant (FCA),[2] which turned out to be one of the most potent adjuvants (5, 6). However, despite its strong efficacy, FCA causes severe local reactions and is considered too toxic for human use (1, 7). The foremost job of an adjuvant is to activate the host immune system. Pattern recognition receptors (*e.g.* Toll-like receptors (TLRs)) present in various antigen-presenting cells like monocytes, macrophages, and dendritic cells play a critical role in innate immune defense by sensing the pathogens (8–11). Considering this, various adjuvant substances have been designed from pathogenic molecules that interact with these pattern recognition receptors. Consequently, TLRs are considered as targets for the design of adjuvants, and many studies have revealed direct co-stimulatory effects of TLR agonists in $CD4^+$ and $CD8^+$ T cells and in B cells in enhancing vaccine-specific responses (12). Ligands for TLR2, TLR3, TLR4, TLR5, TLR7/8, and TLR9 have been evaluated preclinically for their efficacy as components of vaccine adjuvants (13, 14). One adjuvant approved by the Food and Drug Administration is a TLR4 agonist, monophosphoryl lipid A (15, 16). Although promising, many of these TLR agonists are molecules of bacterial origins with a requirement of carrier or vehicle, leaving a chance of undesired side effects. Synthetic TLR4 agonists have been applied as adjuvants in different vaccination procedures (*e.g.* RS09 (17), an LPS mimetic peptide, derived from a phage display library employed in intranasal vaccination against HIV-1, showed lesser side effects with improved adjuvanticity) (18, 19). Recent studies have demonstrated the benefits of adjuvants with the self-assembling property because these molecules can offer multivalency to immunogenic materials (20). Therefore, TLR agonists of totally synthetic nature with the self-assembling property are considered as more appropriate

This work was supported by the CSIR network project BioDiscovery. This is CSIR-CDRI communication number 9759. The authors declare that they have no conflicts of interest with the contents of this article.

This article contains supporting information, Table S1, and Figs. S1–S7.

[1] To whom correspondence should be addressed. Tel.: 091-522-2771940 (ext. 4451); Fax: 091-522-2771941; E-mail: jk_ghosh@cdri.res.in.

[2] The abbreviations used are: FCA, Freund's complete adjuvant; FIA, Freund's incomplete adjuvant; TLR, Toll-like receptor; LPS, lipopolysaccharide; TPP, trehalose-6-phosphate phosphatase; MTT, 3-(4,5-dimethylthiazol-2-yl)-2,5-diphenyltetrazolium bromide; TEM, transmission EM; ThT, thioflavin T; TNF, tumor necrosis factor; IL, interleukin; PMA, phorbol 12-myristate 13-acetate; Ova, ovalbumin; HRP, horseradish peroxidase; IFN, interferon.

Table 1
Sequences, molecular masses, and RP-HPLC retention time of TR-433 and Scr
For TR-433, hydrophobic amino acid residues are shown in boldface type and charged residues in underlined boldface type. The interchanged amino acid residues of Scr are shown in italic type and underlined.

Peptide	Sequence	Calculated mass	Observed mass	RP-HPLC retention time
		Da	*Da*	*min*
TR-433	NLKQMS**E**F**S**V**F**L**S**L**R**NLIYL	2414.86	2414.3	~19–20
Scr	NLK*E*MS*Q*FSV*L*L*N*LR*S*FIYL	2414.86	2414.2	~20–21

candidates for the development of adjuvants and their application as vaccine components (21).

The dimeric crystal structure of TLR4 in complex with adapter protein MD2 and ligand LPS (22) provides the scope of identification of peptides that could interact with these proteins or LPS. Computational studies revealed that a TLR4 segment, TR-433, comprising the amino acid region 433–452 (Table 1), which falls in the dimerization interface of the TLR4–MD2 complex, is involved in intermolecular interactions between two TLR4 molecules and one MD2 molecule. Therefore, we hypothesized that TR-433 could modulate the innate immune responses by interacting with TLR4 and/or MD2. Moreover, when this peptide was incubated with THP-1 cells alone, production of several pro-inflammatory cytokines was observed. The data indicated a pro-inflammatory activity of TR-433, which produced pro-inflammatory cytokines in THP-1 cells presumably by initiating TLR4-activated downstream signaling events. Further, TR-433 readily self-assembled into nanostructures. Altogether, for the first time, we have identified a TLR4 segment that possesses strong self-assembling and pro-inflammatory properties. Hence, the presence of these two distinctive properties (17, 23–25) made TR-433 a suitable candidate for exploring its potential as an adjuvant in vaccination. The present study describes the characterization of TR-433 as an adjuvant for immunization of mice with the antigens ovalbumin and *Brugia malayi* trehalose-6-phosphate phosphatase (TPP) (26), and its comparison with known adjuvants alum and FCA.

Results

Identification of a TLR4 fragment (TR-433)

Molecular docking and MD simulation studies enabled the elucidation of possible interactions among TR-433 and the proteins TLR4 and MD2. From the docked conformations, the docked poses were browsed according to the size of clusters. The largest cluster included 163 docked conformations. Pose number 241 ranked highest of all (*Z* Dock score: 17.96) of the conformations included in this cluster. This conformation was saved and visualized for possible interactions (Fig. S1). The trajectories from 20-ns-long MD simulation of the TLR4–MD2 peptide complex that were saved at 5, 10, 15, and 20 ns, respectively, provided detailed information about the interactions involved. Table S1 lists the residues of TLR4 and MD2 involved in the formation of hydrogen bonds and hydrophobic contacts during the 20-ns-long MD run supporting the docking studies. Previously reported residues (22) like Gln-436 and Glu-439 of TLR4 and Leu-87 and Arg-90 of MD2 were found interacting either through hydrogen bonds or hydrophobic contacts with the peptide, TR-433. Thus, the data indicated that TR-433 falls in the interface of two TLR4 monomers and one MD2 monomer (Fig. S1). This raised a possibility that TR-433 may initiate downstream signaling events by interacting with TLR4–MD2 complex, resulting in the activation of innate immune responses.

The observed mass of TR-433 from MALDI-TOF spectra is close to that of its calculated mass, and HPLC retention time for the purification of the peptide by C-18 column is shown in Table 1.

TR-433 is nontoxic in nature

Hemolytic activity assay suggested that TR-433 exhibited insignificant lysis of human red blood cells up to 200 μM peptide concentration as compared with that of bee venom toxin, melittin (Fig. 1*a*). An MTT assay suggested that TR-433 did not possess significant cytotoxicity toward 3T3, THP-1, and HEK293T cells even up to 200 μM concentration, as evidenced by more than 90% viability of the cells (Fig. 1*b* and Fig. S2*a*). Overall, the data suggested the noncytotoxic nature of the TR-433.

Further, TR-433 at concentrations of 100 μg and 200 μg/animal/day for 3 days were also administered intravenously in the tail of BALB/c mice, and animals were observed for any effects that could lead to mortality for 7 days to investigate its *in vivo* toxicity. No loss of animals was observed, indicating that TR-433 is safe for BALB/c mice at these high peptide concentrations (Fig. 1*c*).

TR-433 induced the production of pro-inflammatory cytokines in a human monocytic cell line, THP-1

MD simulation studies indicate that the TR-433 segment falls within two TLR4 monomers of the TLR4–MD2 dimeric complex. Therefore, it was of interest to examine whether TR-433 peptide could activate TLR4-mediated immunomodulatory events in human monocytic THP-1 cells. TR-433 indeed stimulated THP-1 cells to secrete various pro-inflammatory cytokines like TNFα, IL-1β, and IL-8. LPS-induced cytokine production was followed as a positive control (Fig. 2, *a–c*). Dose-dependent TNFα production in THP-1 was also observed in the presence of TR-433 (Fig. S2*b*). The immunomodulatory property of the peptide was also investigated in a TLR4-deficient HEK293T cell line, transiently transfected with TLR4, CD14, and MD2. Dose-dependent IL-8 production confirmed the pro-inflammatory nature of TR-433 (Fig. 2*d*). The pro-inflammatory nature of TR-433 was further investigated by collecting the sera of BALB/c mice after 4 and 24 h of injection of TR-433 peptide in them. Appreciable IL-6 production, observed in the sera of these BALB/c mice, further confirmed the *in vivo* pro-inflammatory nature of TR-433 (Fig. 2*e*).

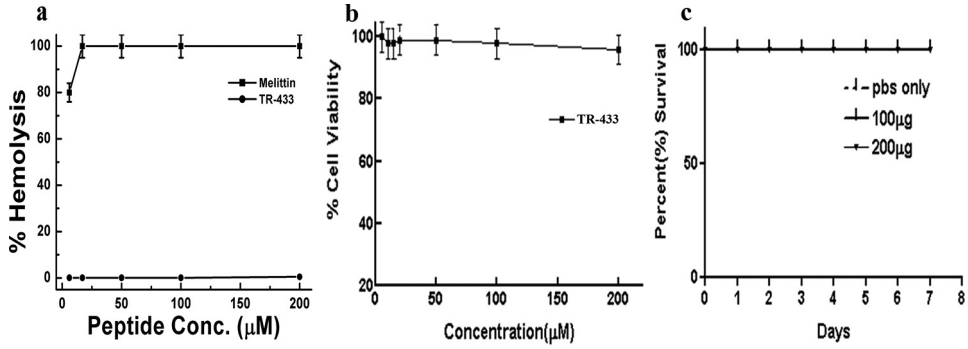

Figure 1. Determination of toxicity of TR-433. *a*, dose-dependent hemolysis of human red blood cells in the presence of TR-433 and melittin. *b*, the viability of murine 3T3 cells in the presence of TR-433 by an MTT assay. Data are representative of the average of three independent experiments ($n = 3$) performed in duplicates. Results are given as mean ± S.E. (*error bars*). *c*, percentage survival of BALB/c mice ($n = 6$) after administering (intravenously) 100 and 200 μg of TR-433/animal/day for 3 days.

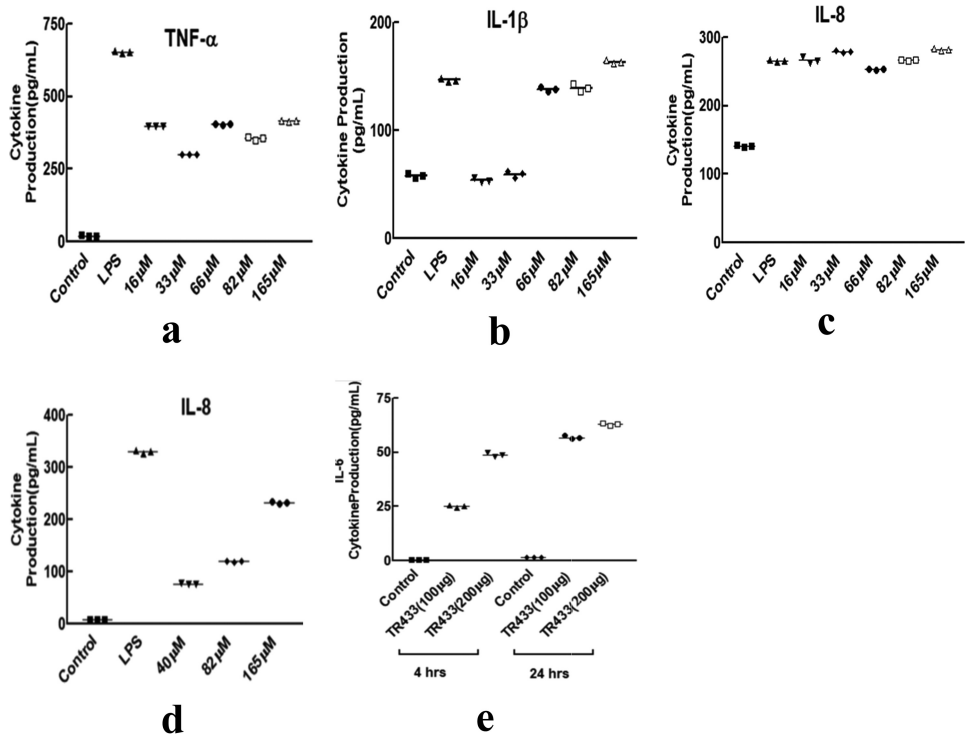

Figure 2. Pro-inflammatory cytokine production. *a–c*, production of TNFα (*a*), IL-1β (*b*), and IL-8 (*c*) at different concentrations of TR-433 in THP-1 cells. Each *data point* is an average of three independent experiments ($n = 3$) performed in duplicates, and results are given as mean ± S.D. (*error bars*). *d*, IL-8 production in transfected HEK293T cells at different concentrations of TR-433. *e*, 100 and 200 μg of TR-433 was injected in mice (intravenously), and sera were collected after 4 and 24 h. IL-6 was quantified by ELISA. Each *data point* is an average of three independent experiments performed in duplicates.

TR-433 possesses the self-assembling property and adopts a nanostructure

The middle of TR-433 contains a hydrophobic stretch (FSV-FLSL) with amino acids that are commonly present in fibril-forming peptides (27). Additionally, at the middle of TR-433, there is a stretch of three hydrophobic residues, namely VFL (28), with a hydrophilic serine residue at its left and right sides followed by again a hydrophobic residue (F/L). The amphipathic arrangement of such strong hydrophobic patches separated by hydrophilic residues seems to assist in self-assembly and nanostructures of peptides (29). Interestingly, from the N terminus, the 7th amino acid of TR-433 is a glutamic acid residue, whereas from the C terminus, the 6th amino acid is an arginine (Table 1). Thus, the presence of opposite charge from the almost equal distance of the N and C termini may propagate the self-assembly of the peptide through intermolecular electrostatic interaction (25). A viscous or gel-like aggregate was formed when TR-433 was dissolved in Milli Q water, within a short period (10 min). Transmission EM (TEM) images of TR-433 showed various aggregated structures. For example, in Fig. 3*A*, *panel a* represents the sheetlike structure of TR-433, whereas the *arrows* in *panels b* and *c* show shorter fibrils of TR-433 of diameter 5 nm. *Panel d* in Fig. 3*A* shows long thick fibrils of diameter 10 nm and large aggregates. Further, with the help of a ζ-sizer, it was found that the peptide formed large aggregates, but the size of the aggregates was not a constant one, as evidenced by the broader peaks in the spectra. The data suggested that the size of the diameter of the aggregate continuously altered among 10, 100, and more than 100 nm (Fig. S3). Moreover, an enormous increase in fluorescence of thioflavin T

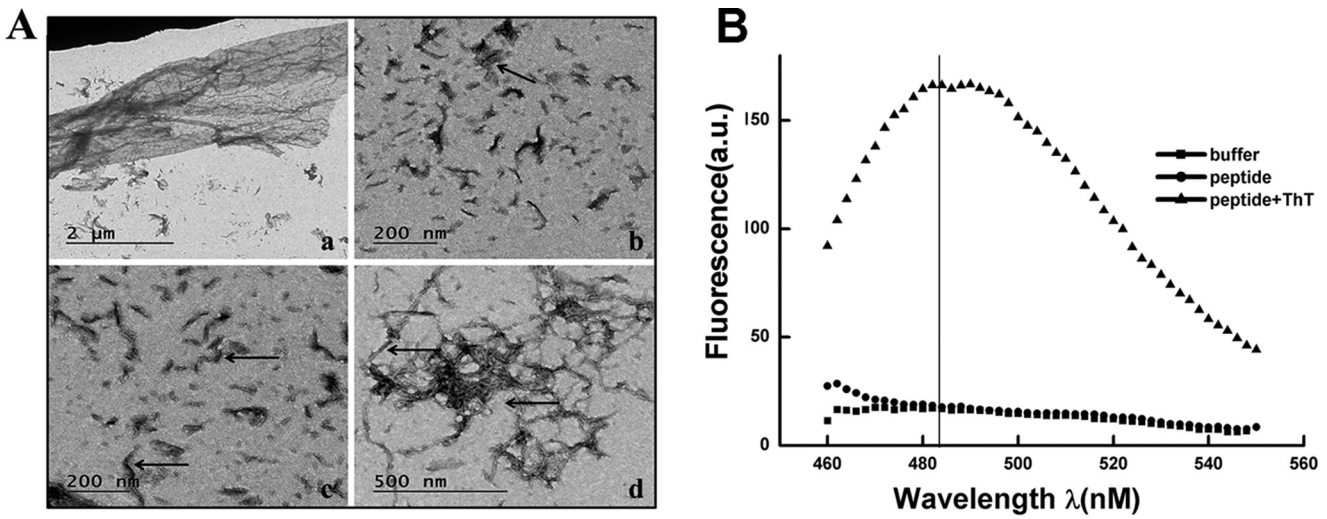

Figure 3. TR-433 possesses the self-assembling property and adopts a nanostructure. *A*, detection of self-assembly property of TR-433 by TEM. *a*, sheet-like structure. *Arrows* in *b* and *c*, shorter fibrils of diameter 5 nm. *d*, long thick fibrils of diameter 10 nm and large aggregates. *B*, ThT fluorescence in the presence of TR-433. Each spectrum is the average of three scans.

(ThT) was observed when it was added to the peptide suspension, suggesting that TR-433 formed fibrillar aggregates (Fig. 3*B*). The FTIR spectrum of the peptide also showed a prominent peak (lowest percentage absorbance) at around 1637 cm^{-1} corresponding to the amide I region, which is an indication of parallel β-sheet structure (30) of the peptide (Fig. S4).

TR-433 is more specific to TLR4 than MD2

Preincubation of the THP-1 cells with TLR4 antibody appreciably attenuated TR-433–induced productions of TNFα and IL-8 (Fig. 4), indicating that this antibody treatment significantly impaired the peptide's efficacy to stimulate pro-inflammatory responses in these cells. However, when the cells were pretreated with MD2 antibody (Fig. 4), the levels of pro-inflammatory cytokine productions in the presence of TR-433 were also reduced but to a lesser extent than that observed with the treatment of TLR4 antibody. The data indicated that TR-433–induced production of pro-inflammatory responses is more associated with TLR4 than MD2. Overall, the results suggested that TR-433 acted as a partial TLR4 agonist and induced the production of pro-inflammatory cytokines in THP-1 cells.

TR-433 activates NF-κB and mitogen-activated protein kinase pathways downstream of TLR4

Translocation of NF-κB to the nucleus is a key event for the production of pro-inflammatory cytokines by the innate immune system and was therefore examined in the absence and presence of TR-433 in PMA-stimulated THP-1 cells. Immunoblotting experiments by employing NF-κB p65 antibody suggested that TR-433 induced the translocation of NF-κB to the nucleus of these cells. This translocation was stopped by the addition of anti-TLR4 antibody, 2 h prior to the addition of TR-433 (Fig. 5*a*). Further, it was supported by the fact that TR-433 also induced the degradation of IκBα (Fig. 5*b*). Media and LPS served as −ve and +ve controls, respectively.

Additionally, TR-433 enhanced p38 phosphorylation in PMA-stimulated THP-1 cells (Fig. 5*c*). However, the addition of anti-TLR4 antibody to PMA-stimulated THP-1 cells for 1 h prior to peptide treatment significantly inhibited TR-433–induced p38 phosphorylation (Fig. 5*c*).

However, a pretreatment with a nonspecific IgG antibody did not show any effect on TR-433–induced NF-κB translocation. Overall data indicated that TR-433–induced production of pro-inflammatory responses and NF-κB translocation is more associated with TLR4 (Fig. 5*d*).

To further confirm this translocation (*i.e.* whether TR-433 activates NF-κB), HEK293T cells, transiently expressing TLR4, MD2, and CD14, were transfected with an NF-κB luciferase reporter construct. Transfected HEK293T cells without the treatment of TR-433 served as control, and untransfected HEK293T served as mock control. TR-433 induced a dose-dependent increase in luciferase activity in HEK293T-TLR4-MD2-CD14 cells but not in transfected HEK293T control cells (Fig. S5, *a* and *b*). IL-8 production in TLR4-, MD2-, and CD14-transfected HEK293T cells also increased following the stimulation with TR-433(Fig. S5*c*), linking activation of the NF-κB pathway with cytokine production. This translocation was also inhibited in the presence of anti-TLR4 antibody (Fig. S5).The role of NF-κB activation and involvement of TLR4 in the activity of TR-433 was further investigated by looking into the activity of this peptide in HEK293T cells after transfection with MD2 and CD14. The absence of any significant IL-8 production in these cells (Fig. S5*e*) verified the requirement of TLR4, the lack of which presumably abrogated NF-κB activation and thus activity of TR-433 in these cells. Production of IL-8 even in the presence of nonspecific IgG antibody (Fig. S5*f*) in HEK293T cells transfected with TLR4-CD14-MD2 further corroborated the specificity of TR-433 toward TLR4 and thus the activity of TR-433 in these cells. A dose response of TR-433 was checked in untransfected cells, and the peptide was found to be inert toward them (Fig. S5*d*).

IgG titers elicited by TR-433 with ovalbumin/r-Tpp

Looking at the amino acid sequence and attributes of TR-433, it was considered as a suitable candidate for examina-

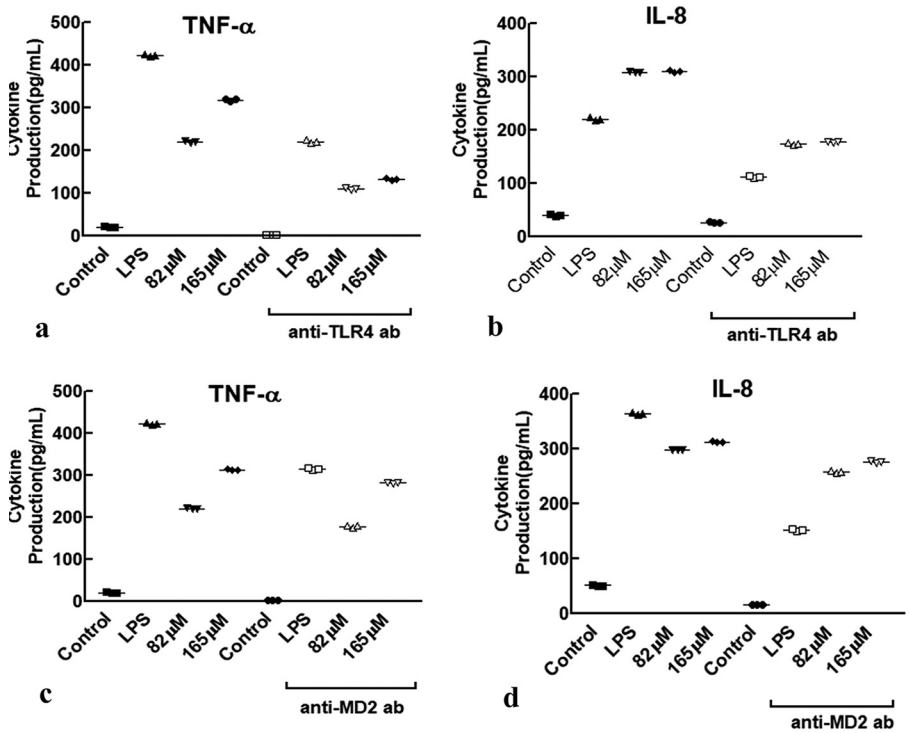

Figure 4. TR-433 is more specific to TLR4 than MD2. THP-1 cells were treated with or without anti-TLR4 (*a* and *b*) and anti-MD2 antibody (*c* and *d*) (2.5 mg/ml) in the presence of TR-433, and cytokines were quantified by ELISA. LPS and untreated cells served as positive and negative controls, respectively. Each *data point* is an average of three independent experiments ($n = 3$) performed in duplicates, and results are given as mean ± S.D. (*error bars*).

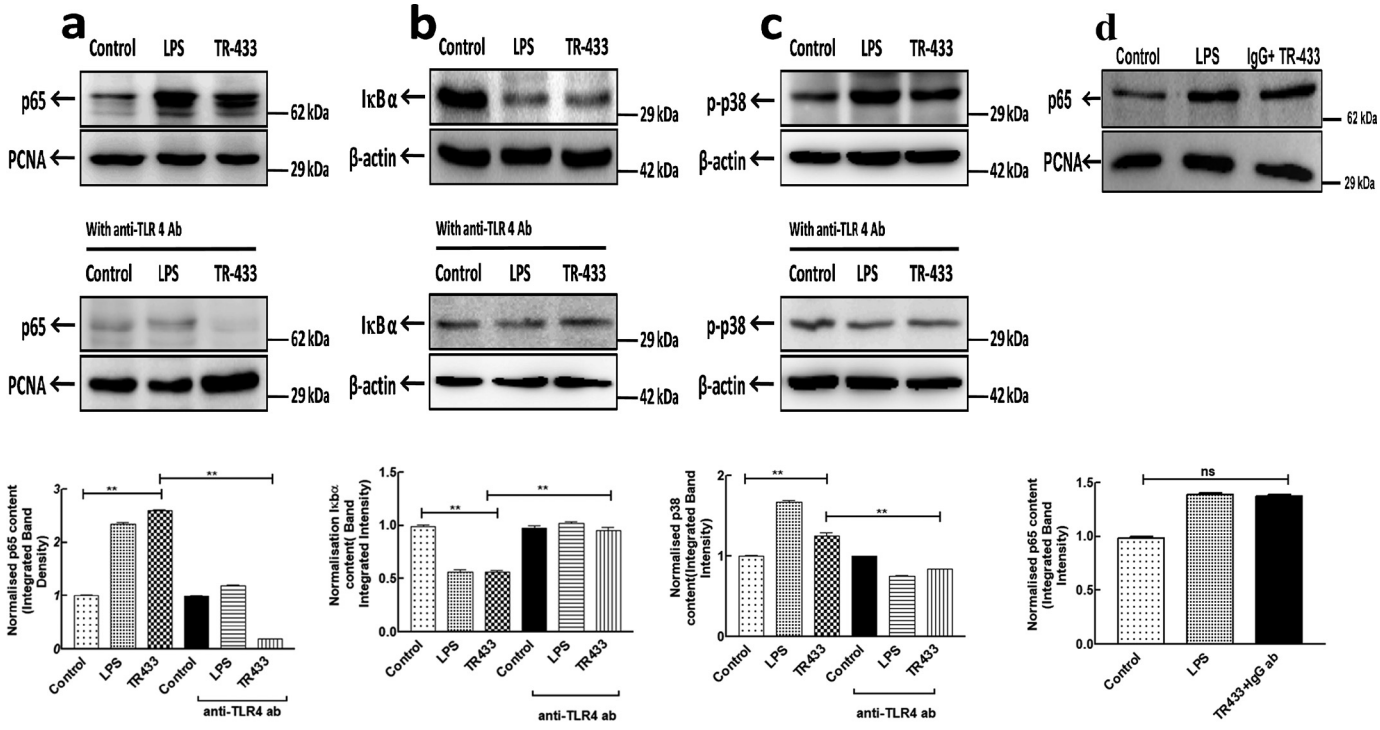

Figure 5. TR-433 activates NF-κB and mitogen-activated protein kinase pathways. PMA-stimulated THP-1 cells (1×10^6) were treated with TR-433 in the presence and absence of anti-TLR4 antibody (2.5 mg ml^{-1}). *a*, nuclear fractions were assessed for NF-κB translocation. *b*, cytoplasmic fractions were assessed for IκBα degradation. *c*, phosphorylation of p38 was assessed in cell lysates. *d*, nuclear fractions were assessed for NF-κB translocation in the presence of anti-IgG antibody (2.5 mg ml^{-1}). Proliferating cell nuclear antigen (*PCNA*) and β-actin served as loading controls, respectively. Each *data point* is representative of three independent experiments ($n = 3$). The *middle lane* includes fractions preincubated with anti-TLR4 antibody. The *last lane* shows the corresponding normalized integrated band intensity. Statistical analysis was carried out using one-way analysis of variance using Turkey's test (**, $p \leq 0.01$; ns, not significant). *Error bars*, S.D.

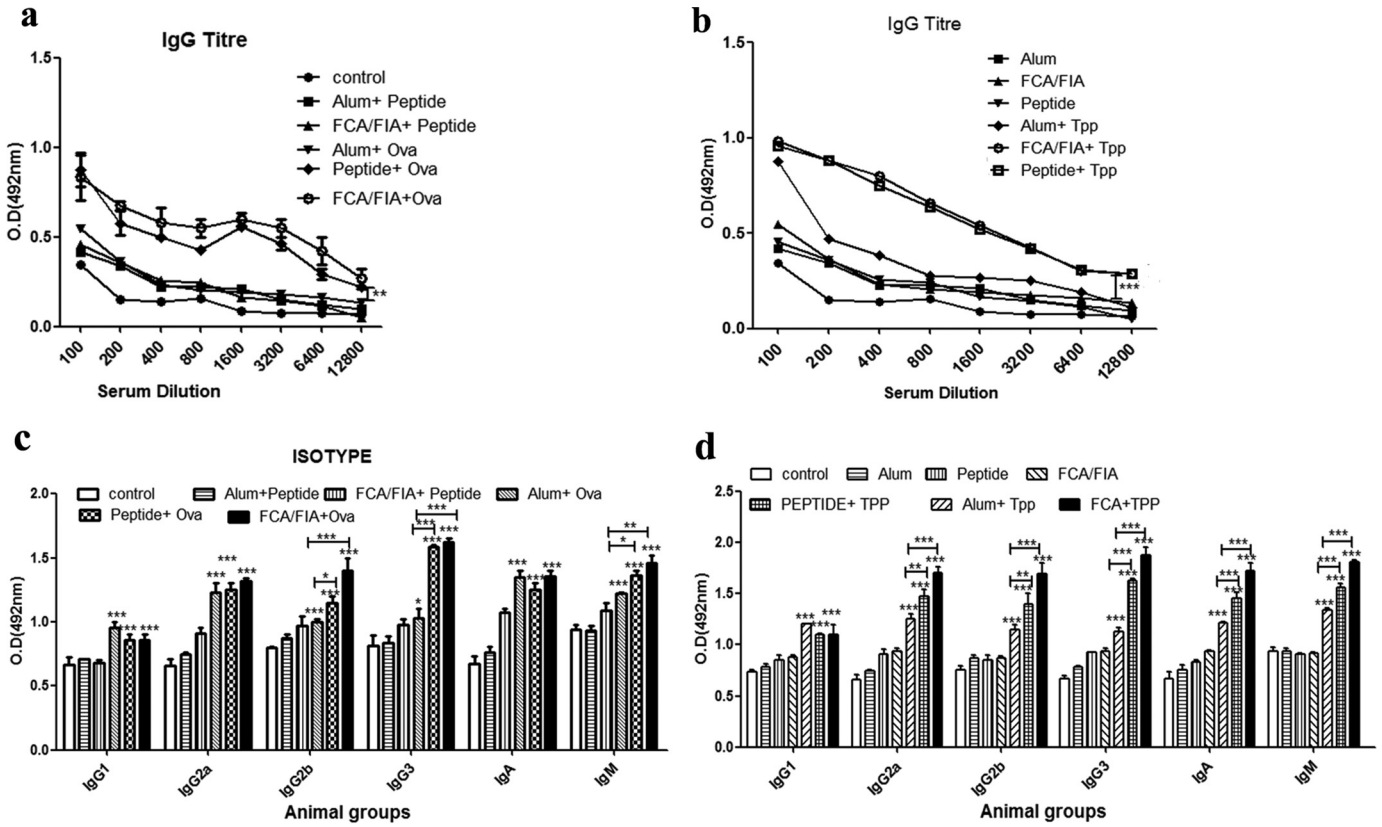

Figure 6. IgG titers and isotyping of immune responses elicited by the peptide with ovalbumin/r-Tpp. *a* and *b*, mice were divided into 12 different experimental groups, each having five animals, and experiments were repeated twice independently ($n = 2$). Group 1 mice were left untreated (control group); whereas group 2 mice were immunized with alum alone. Groups 3 and 4 were immunized with TR-433 (50 μg) and FCA/FIA alone. Groups 5–7 were immunized with 25 μg of Ova with alum, TR-433, and FCA, respectively. Groups 8–10 were immunized with 25 μg of TPP with alum, TR-433, and FCA, respectively. Groups 11 and 12 were treated with TR-433 along with either alum and FCA/FIA. One week after the final booster dose, mice were killed. Splenocytes and blood were collected, and IgG titers were elicited by ELISA. *c* and *d*, antibody isotypes were measured by ELISA in duplicates. Statistical analysis was carried out using one-way analysis of variance using Dunnett's test. *, $p \leq 0.05$; **, $p \leq 0.01$; ***, $p \leq 0.001$. *Error bars*, S.E.

tion of its adjuvant property. To evaluate the adjuvant-like activity of TR-433, 50 μg of the peptide was mixed with 25 μg (23, 31–33) of modeled antigen, ovalbumin, which is mildly immunogenic, in 100 μl of PBS, and four mice per group were immunized with it. Alum and FCA with the ovalbumin were used as positive control, whereas PBS, alum, and FCA alone served as negative controls. Injections were administered on days 0, 14, 21; sera were collected on day 28; and titers were measured by the ELISA method. The results showed that peptide elicited an adjuvant-like property that was at a significantly elevated level as compared with that in the presence of alum and was very similar to that of FCA. The highest IgG titer was at a dilution of 1600. To examine whether TR-433 itself can produce IgG titer, it was injected in mice in combination with either FCA/FIA or alum. IgG titers of peptide + FCA/FIA and peptide + alum were analyzed and compared with that of ovalbumin, injected with standard adjuvants. Results showed that TR-433 did not show any significant increase in IgG titer as compared with ovalbumin in ELISA experiments (Fig. 6*a*).

To further explore the adjuvant-like activity of TR-433, filarial antigenic protein, r-Tpp, was administered in mice with this peptide, and for a comparative study, this protein was also administered in combination with alum or FCA/FIA (34). The results indicated that TPP + FCA/FIA and Tpp + TR-433 administered in mice generated significantly higher titers with specific IgG antibodies at higher serum dilutions as compared with that observed with Tpp + alum ($p < 0.001$) (Fig. 6*b*).

Isotyping of immune responses

To characterize the immune response generated by the antigenic proteins in the presence of TR-433, the isotypes of antisera were evaluated by ELISA experiments. The results indicated that TR-433 induced the generation of IgG1, IgG2a, IgG3, and IgM responses as a result of immunization of mice with ovalbumin and filarial antigen TPP. In particular, TR-433 elicited significantly high levels of IgG2a, IgG3, and IgM responses as compared with the other isotypes, suggesting antigen-specific T-cell responses. Higher levels of IgG2a than IgG1 (ratio >1) illustrated that TR-433 could preferentially induce type 1 helper T cell (T_h1) response over type 2 T-helper cell (T_h2) response (Fig. 6, *c* and *d*) (25).

Characterization of extracellular cytokines as a result of immunization of mice with Ova/r-Bm-TPP in the presence of TR-433

To further characterize the phenotype of the developing immune response (T_h1 *versus* T_h2) generated by Ova/r-Bm-TPP in the presence of TR-433, splenocytes from the control and immunized groups were stimulated *in vitro* with Ova or

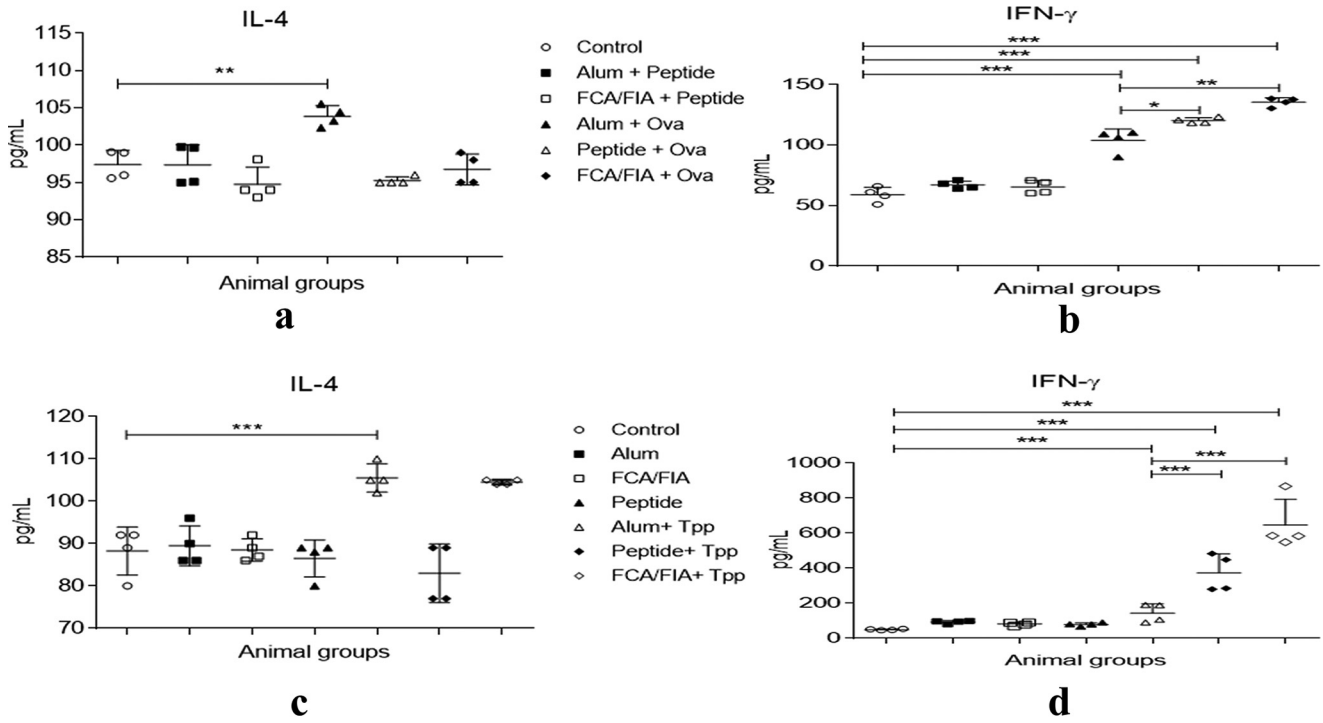

Figure 7. Characterization of extracellular cytokines as a result of immunization of mice with Ova/r-Bm-TPP in the presence of TR-433. 1×10^6 splenocytes were cultured for 48 h in the presence of Ova and r-Bm-TPP in cRPMI at 37 °C. Supernatants were collected, and levels of cytokines IFN-γ (*b* and *d*) and IL-4 (*a* and *c*) were estimated in the culture supernatants of splenocytes in duplicates in two independent experiments ($n = 2$). Statistical analysis was carried out using one-way analysis of variance using Dunnett's test (*, $p \leq 0.05$; **, $p \leq 0.01$; ***, $p \leq 0.001$). *Error bars*, S.E.

TPP for 48 h, and levels of IFN-γ, IL-4, and IL-10 were measured in cell culture supernatants. A significant increase in the levels of IFN-γ, but not of IL-4 and IL-10, was observed in the two immunized groups of splenocytes obtained from the mice that were immunized in the presence of TR-433, suggesting a polarization toward the T_h1 phenotype (Fig. 7 (*a* and *c*) and Fig. S6). The T_h1 subset helps in the production of cytokine IFN-γ, thus eliciting cellular immunity through the $CD4^+$ population (Fig. 7, *b* and *d*). The results also showed the cellular responses that were induced by known adjuvants, alum and FCA/FIA, during immunization. For example, alum with either TPP or Ova predominantly induced IL-4 and IL-10 response over IFN-γ, suggesting its preference for a T_h2-specific cellular response (Fig. 7 (*a* and *c*) and Fig. S6), whereas FCA/FIA showed a significant production of IFN-γ, indicating Th1-specific responses. Overall, the data indicated that TR-433 resembled FCA/FIA rather than alum in inducing cellular responses during immunization.

TR-433 adjuvant activity depends on T-bet expression

To further confirm the type of T-cell response generated during immunization of mice with ovalbumin and TPP in the presence of TR-433, we studied mRNA expressions of the T-bet and GATA-3 transcription factors in splenocytes, which regulate T_h1 and T_h2 response, respectively (35, 36). The results of the mRNA expressions were analyzed (Fig. 8, *a* and *b*) and indicated that the expression of T-bet dominates over GATA-3. Thus, the dominance of T_h1 response over T_h2 response reconfirmed that TR-433 activated T_h1-specific immune response during the immunization of mice with ovalbumin and TPP.

Discussion

Food and Drug Administration–approved adjuvants are limited to aluminum-based salts and monophosphoryl lipid A, a bacterial product (37). Strong adjuvants like FCA and liposomes have been reported in the literature but have not been recommended for human application. This is because the traditional carriers employed for these adjuvants often have low stability, low encapsulation efficiency, and cross-reactivity with the antigen or undesired side effects, including cytotoxicity, autoimmunity, etc. (38, 39). Recent results suggest that hydrophilic polyester-based nanoparticles in combination with a TLR3 ligand can efficiently act as an adjuvant and induce the strong T-cell response of a peptide antigen derived from human papillomavirus (7). Thus, there is a demand for new adjuvants with versatile functions like intelligent release and biocompatibility with the immune system to enhance the vaccination (40).

Toward this, the present results show the identification of a short peptide segment from human TLR4 protein encompassing the amino acid region 433–452 (TR-433), which self-assembled into a nanofibrillar structure, acted as a partial TLR4 agonist, and induced significant immune responses when injected in mice in a mixture with ovalbumin and filarial antigen protein TPP. The ability to adopt nanostructures as well as to act as a TLR4 agonist for a single molecule is the distinction of this TLR4-derived peptide, TR-433, that seemed to enable it to act as a potent adjuvant.

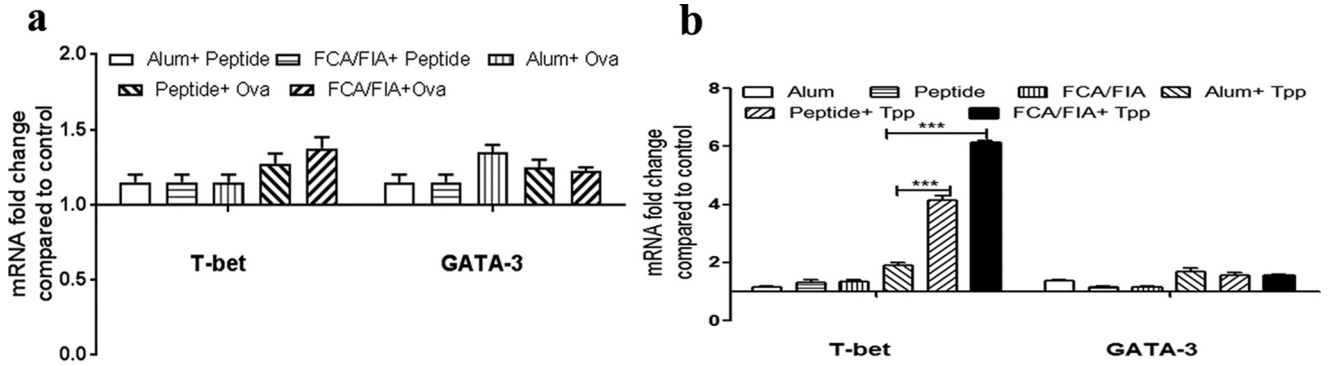

Figure 8. TR-433 adjuvant activity depends on T-bet expression. mRNA expressions of T-bet and GATA-3 were analyzed in splenocytes in duplicates in two independent experiments ($n = 2$). Mouse glyceraldehyde-3-phosphate dehydrogenase was used as an endogenous control, and relative -fold change was determined by the comparative ΔCT method. Statistical analysis was carried out using one-way analysis of variance using Dunnett's test. *, $p \leq 0.05$; **, $p \leq 0.01$; ***, $p \leq 0.001$. *Error bars*, S.E.

TR-433 showed its significant nontoxic nature in *in vitro* (Fig. 1, *a* and *b*) and *in vivo* experiments with mice (Fig. 1*c*), which is an important criterion for the application of a biomaterial as an adjuvant. TR-433 displayed its strong adjuvanticity at 50 μg/mouse (~25-g mice), whereas in *in vivo* toxicity studies of the peptide showed its nontoxic nature when it was administered in mice for 200 μg/day/mouse for 3 days. Thus, the results indicated that TR-433 showed its adjuvant property well below the concentration at which it could exert any toxicity in mice.

Computational studies (Fig. S1 and Table S1) revealed that TR-433 is located in the dimerization interface of the TLR4–MD2 complex and thus may interact with the innate immune system and activate downstream signaling events. Moreover, it indicated that TR-433 could be more associated with TLR4 than MD2. Experiments performed with TLR4 and MD2 antibody supported this notion (Fig. 4). TLR4 is one of the most important pattern recognition receptors that recognize pathogen-associated molecular patterns and has been targeted to activate the innate and adaptive immune responses in the presence of an antigenic protein and also to design molecules with adjuvant-like activities (17, 41, 42). Results indicated that TR-433 induced the translocation of NF-κB into the nucleus of PMA-stimulated THP-1 cells and produced the pro-inflammatory cytokines TNFα, IL-8, and IL-1β in these cells (Fig. 2, *a*–*c*). Further, TR-433 also induced the same events in TLR4-MD2-CD14–transfected, TLR4-deficient HEK293T cell lines (Fig. S5), whereas no cytokine production was observed in HEK293T cells, transfected with MD2 and CD14 (Fig. S5). Interestingly, a pretreatment of TLR4 antibody significantly antagonized the TR-433–induced production of pro-inflammatory cytokines in THP-1 cells, and almost no alteration in the production of cytokines with pretreatment of nonspecific IgG antibody suggested the TLR4 specificity of this peptide (Fig. S5*f*) as revealed by computational studies (Fig. S1) also. To understand the specificity of the TLR4-derived peptide, TR-433, in inducing pro-inflammatory responses in THP-1 cells, a scrambled peptide (Scr) was designed. In Scr key residues of TR-433 involved in the molecular interactions with TLR4 in the computation model were interchanged, as marked in the sequence (Table 1). Thus, the number of amino acids and composition of Scr remained the same as for the parent peptide, TR-433. Interestingly, when TR-433 was replaced with its scrambled version, Scr, and its pro-inflammatory responses were investigated in THP-1 cells, the peptide failed to induce appreciable production of pro-inflammatory cytokines in these cells (Fig. S7). The inactivity of Scr peptide, despite having the same amino acid composition as TR-433, suggested a crucial role of the amino acid sequence of TR-433 in its pro-inflammatory responses. Further, Scr also failed to induce the translocation of NF-κB subunit, p65, appreciably to the nucleus of PMA-treated THP-1 cells (Fig. S7).

TR-433 self-assembled and adopted a fibrillar kind of nanostructure in the range of 100 nm (Fig. S3), which could efficiently enter the lymphatic system and be internalized by the antigen-presenting cells (43) (Fig. 3). The self-assembling property of the TR-433 was further corroborated with its β-sheet structure, as observed by FTIR spectroscopy (30) (Fig. S4). Recent results reported that coupling of a peptide epitope to the N-terminal of a self-assembling peptide with the ability to adopt fibrillar structure generated robust antibody production, demonstrating the adjuvanting capability of such peptide (44). However, in the present study, there was no requirement of covalent coupling of TR-433 with any peptide/antigen epitope, and it elicited the production of significant IgG titer in the presence of whole-protein ovalbumin and filarial protein TPP. Therefore, when TR-433 is employed as an adjuvant, there is no need for identification of the epitopic region of an antigenic protein for its antibody production. Thus, TR-433 seems to have more advantage in terms of its ease of usage compared with the recently reported adjuvant molecules (*e.g.* self-assembling peptide) (20), lipopeptide (45, 46), coiled-coil oligomerization domains (47), and polymers (20, 48). It is evident from the broader peaks of the dynamic light scattering study (Fig. S3) that aggregated TR-433 possessed multiple aggregation states and seemed to move between more and less aggregated states; TEM studies also confirm this notion (Fig. 3*A*). It has been reported previously that a balance between aggregation and disaggregation in a peptide helps in the slow, controlled, and better release of antigens to the antigen-presenting cells and macrophages (25), whereas the presence of a pro-inflammatory property makes it an immune stimulant that helps in the generation of a better immune response.

Alum induces both cellular and humoral immune responses. Th2 cellular response is characterized by the production of cytokines IL-4 and IL-10, and humoral responses are characterized by the production of IgG antibodies (49). Moreover, as observed in the present study (Fig. 7 and Fig. S6), alum preferentially activates T_h2 cells that facilitate the differentiation of B cells, leading to the production of antibodies IgG1 and IgE, causing local and systemic side effects, including sterile abscesses, eosinophilia, myofacitis, and sometimes neurotoxicity. Therefore, alum is not considered an appropriate adjuvant for vaccination against many diseases (1, 50). FCA/FIA produces strong T_h1 and T_h17 (38) cell responses that are dependent on the mycobacterial component present in it. However, the presence of its hallmarks like focal necrosis lesions and a granulomatous inflammatory response leading to foamy oil-filled macrophages at the injection site makes it also an inappropriate adjuvant for application in immunization (51). Thus, the findings of appropriate adjuvants that provide protection against pathogens as well as a safety against these mentioned drawbacks are very crucial and needed. It has been reported that most T_h1 polarized responses are elicited by the adjuvants that behave as agonists of TLR3, TLR4, TLR7, TLR8, and TLR9, which corroborates the present study (13). Interferon-γ (IFN-γ) is a T_h1-specific cytokine that is crucial in macrophage activation (52). TR-433 produced an appreciable amount of IgG2a titers and IFN-γ that was further supported by the expression of T-bet transcription factors (Fig. 8), thereby indicating the induction of T_h1-specific immune responses during immunization of mice with ovalbumin or TPP by employing TR-433 as an adjuvant. Thus, the data suggested that TR-433 can elicit cellular immunity through a $CD4^+$ T-cell population. Overall, TR-433 can also provide protective cellular immune response, which is a requirement for an ideal adjuvant. Recently, a TLR4 agonist peptide, RS09, was either chemically conjugated or physically mixed with a polymer, namely DEG-PEI, and then complexed with rAd5, which encodes HIV group-specific antigen (18). Intranasal administration of this polymer-coated rAd5 vaccine in mice yielded stronger cytotoxic T lymphocyte responses and group-specific antigen–specific IgG titers than naked rAd5 (18). The results suggested a crucial role of chemical conjugation or physical mixing of TLR4 agonist peptide, RS09, with polymer DEG-PEI in augmenting immunogenicity of the rAd5 vaccine (18).

Because it is totally synthetic in nature, TR-433 possesses a definitive advantage of biocompatibility and leaves no chance of bacterial contamination and excludes associated side effects. Moreover, TR-433 did not produce any IgG titer of its own. The current data open up the opportunity of investigating the adjuvanting capability of TR-433 with other antigens. Further, the results raise a possibility of exploring the identification of new peptide adjuvants from the interface of the TLR4–MD2 dimer that can be used in biomedical applications.

Experimental procedures

Peptide synthesis and purification

This is described in the supporting information.

Assay of hemolytic activity of the peptides

This is described in the supporting information.

Docking studies

Docking was performed using the docking program ZDOCK (53) included in Discovery Studio. ZDOCK is a rigid-body docking program and fortunately requires minimal information about the binding site. Crystal structure coordinates of the TLR4–MD2–LPS complex (Protein Data Bank code 3FXI) were obtained from the Protein Data Bank. From this structure, ligands including LPS were removed, and the resulting structure was considered for the protein preparation protocol "Prepare Protein" of Discovery Studio. Similarly, the peptide was also subjected to a similar protocol of protein preparation. The output files obtained at this stage were used for docking considering the default parameters. Molecular visualization was aided by a visualization tool, UCSF-Chimera (version 1.8.1) (54). LIGPLOT$^+$ (version 1.4.5) (55) was considered to draw DIMPLOT and identify the hydrophobic contacts, hydrogen bonds between the protein chains within the complex.

MD simulations

To evaluate the stability of the docked complex, molecular dynamics studies were performed. The Groningen MAchine for Chemical Simulations (GROMACS) version 5.0.7 package (56) was considered for this study. The topology of the proteins was prepared considering the "GROMOS96 43a1" force field (57). In total, 27 sodium ions were added to neutralize the system because the solvated system had a net charge of −27. Later, the system was minimized using the steepest descent method. The minimized system was subjected to an equilibration run. Finally, the equilibrated system was subjected to a 20-ns-long molecular dynamics run. For a detailed analysis of interactions involved during the simulation period, the trajectories of the TLR4–MD2–peptide complex were saved at 5, 10, 15, and 20 ns.

Cell preparation and stimulation

THP-1, the human embryonic kidney cell line HEK293T, and 3T3 cell lines obtained from the CSIR-Central Drug Research Institute, Lucknow cell line repository were cultured in RPMI 1640 medium (Invitrogen) and DMEM (Sigma), respectively, supplemented with 10% fetal bovine serum (Gibco), 10 mM HEPES (Invitrogen), and Anti-Anti 100 X (antibiotic-antimycotic, 15240, Invitrogen).

Measurement of cytokine expression levels in supernatant

ELISAs were performed to estimate the secreted TNFα, IL-8, and IL-1β in LPS- and peptide-treated cells after a 4–6-h incubation. Media and LPS-treated cells served as negative and positive controls, respectively. The experiments were performed according to the manufacturer's protocol (BD Biosciences).

SDS-PAGE and Western blotting

Nuclear and cytoplasmic extracts from PMA-stimulated THP-1 macrophages (5×10^5) treated with peptide TR-433 and LPS, respectively, were prepared using lysis buffer A (20 mM

Tris, pH 8.0, 10 mM NaCl, 3 mM $MgCl_2$, 0.1% Nonidet P-40, 10% glycerol, 0.2 mM EDTA with protease and phosphatase inhibitors) and lysis buffer C (20 mM Tris, pH 8.0, 400 mM NaCl, 0.2 mM EDTA, 20% glycerol, 1 mM DTT with protease and phosphatase inhibitors), and 40 μg of proteins were fractionated on 10% SDS-polyacrylamide gel and then transferred to nitrocellulose membrane. Blots were blocked in 5% skimmed milk in 1× PBST (20 mM Tris base, 150 mM NaCl, 0.05% (v/v) Tween 20) for 2 h at room temperature. Further, blots were then incubated with primary antibodies human anti-NF-κB p65, IκBα, proliferating cell nuclear antigen (Cell Signaling Technology), and β-actin (1:1000 in 1× PBST) overnight at 4 °C. The next day, blots were washed three times with 1× PBST followed by incubation with HRP-linked, secondary anti-rabbit IgG antibody (1:5000 in 1× TBST), followed by three washes with 1× TBST. Blots were then developed immediately using chemiluminescence HRP substrate (ECL, Millipore) in an ImageQuant LAS 4010 imager (GE Healthcare).

For the detection of phosphorylation of p38, whole-cell extracts were made. PMA-treated THP-1 macrophages (5×10^5) were lysed in radioimmune precipitation assay lysis buffer (1% (w/w) Nonidet P-40, 0.5% (w/v) sodium deoxycholate, 0.1% (w/v) SDS, 0.15 M NaCl, 5 mM EDTA, 1 mM DTT, phosphatase and protease inhibitors) and subjected to immunoblotting with specific primary antibody of p-p38, followed by incubation in HRP-conjugated secondary anti-rabbit IgG antibody developed immediately using chemiluminescence HRP substrate in ImageQuant LAS 4010. All antibodies were purchased from Cell Signaling Technology.

Transfection of HEK293T cells and luciferase assay

HEK293T cells were plated at a concentration of 1×10^5 cells/well in 24-well plates. Expression plasmids FLAG-CMV1-TLR4 (5 ng/well), pcDNA3-CD14 (15 ng/well), pEFBos-HA-MD2 (5 ng/well) together with NF-κb-Luc (100 ng/well), and pRL-TK (10 ng/well) were transiently transfected (58) with Lipofectamine 2000 (Invitrogen) reagent according to the manufacturer's protocol. The total amount of transfected DNA was kept constant with empty vector. 4 h posttransfection, complete medium (Dulbecco's modified Eagle's medium supplemented with 10% fetal bovine serum and antibiotics) was added to the cells. 24 h posttransfection, cells were treated with peptide and LPS with respective concentrations for 16–20 h prior to lysate preparation. After 16 h of treatment, growth media were removed from cultured cells, 100 ml of the passive lysis buffer was dispensed in each cultured well, and luciferase activity was measured with a Dual-Luciferase® reporter assay kit (Promega) using a luminometer (GLOMAX). All data are presented as the means ± S.D. of triplicate well readings, normalized to a value of 1.0 compared with an unstimulated negative control.

TEM

This is described in the supporting information.

Dynamic light scattering

This is described in the supporting information.

ThT assay

This is described in the supporting information.

Attenuated total reflectance–FTIR

This is described in the supporting information.

Animals

Animals for experiments were provided by the National Laboratory Animal Centre, CSIR-CDRI (Lucknow). All animal procedures were carried out according to the guidelines of the Committee for the Purpose of Control and Supervision of Experiments on Animals (CPCSEA), Government of India, duly approved by the Institutional Animal Ethics Committee (approval no. IAEC/2011/145 dated March 7, 2014) and National Laboratory Animal Centre (Lucknow).

In vivo adjuvant studies, treatment of mice

To elucidate the potential of peptide TR-433 as an adjuvant in the mice, mice were divided into 12 different experimental groups, each having five animals, and the experiment was done twice independently. (For more details, see the supporting information).

Serum IgG and antibody isotypes

IgG antibodies and antibody isotypes to Ova/TPP were determined in the mice sera by indirect ELISA as described elsewhere (26). (For more details, see the supporting information).

Measurement of cytokines

To determine cytokine levels in the splenocytes from different groups of treated mice, 1×10^6 splenocytes were cultured for 48 h in the presence of Ova/Tpp in cRPMI at 37 °C. Thereafter, supernatant was collected, and levels of cytokines IFN-γ IL-4 and IL-10 were estimated in the culture supernatants of splenocytes using commercially available ELISA kits (BioLegend, San Diego, CA).

Real-time RT-PCR

Real-time RT-PCR analysis of splenocytes was carried out as described earlier (59).

Statistical analysis: adjuvant experiments

Parasite load was calculated from at least five different animals/group. For all other experiments, data were collected from at least five animals/group, and the experiment was repeated twice. Statistical analysis was carried out using one-way analysis of variance using Dunnett's test. *, $p \leq 0.05$; **, $p \leq 0.01$; ***, $p \leq 0.001$ between different groups (alum and FCA/FIA).

Author contributions—A. T. and J. K. G. conceptualization; J. K. G. design of peptides; A. T., M. P., , M. K. H., and M. S. investigation; A. T., M. P., M. K. H., S. A., M. S., T. A., and M. I. S. methodology; A. T., M. P., K. M., S. M. B., and J. K. G. writing-original draft; A. T., M. P., M. I. S., K. M., S. M. B., and J. K. G. formal analysis; M. I. S, K. M., S. M. B., and J. K. G. supervision; K. M., S. M. B., and J. K. G. writing-review and editing.

Acknowledgments—We are thankful to Dr. Jagdeshwar Reddy Thota and R. Khanna (Sophisticated Analytical Instrumentation Facility (SAIF)) for assistance in recording the MALDI-TOF mass and FTIR spectra, respectively. The Pharmaceutics Division, CSIR-CDRI, is thankfully acknowledged for the use of ζ-sizer. We also thankfully acknowledge the National Laboratory Animal Centre (Lucknow) for providing the animals. We thankfully acknowledge Prof. Douglas Golenbock (Medicine Department, University of Massachusetts Medical School, Worcester, MA) for kindly sending the expression vectors, FLAG-pCMVTLR4, pEF-Bos-HAMD2, and pcDNA3-His CD14, and also Dr. Anila Dwivedi (Endocrinology Division CSIR-CDRI, Lucknow) for NF-κB-Luc, pRL-TK control, and pcDNA3 empty vectors. Prof. Surajit Bhattacharyya (Nanyang Technological University, Singapore) is thankfully acknowledged for discussion of the manuscript. We are very thankful to the present and past directors of CSIR-Central Drug Research Institute for support.

References

1. Petrovsky, N., and Aguilar, J. C. (2004) Vaccine adjuvants: current state and future trends. *Immunol. Cell Biol.* **82,** 488–496 CrossRef Medline
2. Schijns, V. E. (2000) Immunological concepts of vaccine adjuvant activity. *Curr. Opin. Immunol.* **12,** 456–463 CrossRef Medline
3. Brown, F., and Haaheim, L. R. (1998) *Modulation of the Immune Response to Vaccine Antigens*, pp. 13–18, Karger, Basel, Switzerland
4. Vogel, F. R., and Powell, M. F. (1995) A summary compendium of vaccine adjuvants and excipients. In: *Vaccine Design: The Subunit and Adjuvant Approach* (Powell, M. F., and Newman, M. J., eds) pp. 234–250, Plenum Publishing Corp., New York
5. Freund, J., C. J., Hosmer, E. P. (1937) Sensitization and antibody formation after injection of tubercle bacilli and paraffin oil. *Proc. Soc. Exp. Biol. Medical* **37,** 509–513 CrossRef
6. Stuart-Harris, C. H. (1969) Adjuvant influenza vaccines. *Bull. World Health Org.* **41,** 617–621 Medline
7. Rahimian, S., Fransen, M. F., Kleinovink, J. W., Christensen, J. R., Amidi, M., Hennink, W. E., and Ossendorp, F. (2015) Polymeric nanoparticles for co-delivery of synthetic long peptide antigen and poly IC as therapeutic cancer vaccine formulation. *J. Control Release* **203,** 16–22 CrossRef Medline
8. Duthie, M. S., Windish, H. P., Fox, C. B., and Reed, S. G. (2011) Use of defined TLR ligands as adjuvants within human vaccines. *Immunol. Rev.* **239,** 178–196 CrossRef Medline
9. Beutler, B. A. (2009) TLRs and innate immunity. *Blood* **113,** 1399–1407 Medline
10. Stoll, L. L., Denning, G. M., and Weintraub, N. L. (2006) Endotoxin, TLR4 signaling and vascular inflammation: potential therapeutic targets in cardiovascular disease. *Curr. Pharm. Des.* **12,** 4229–4245 CrossRef Medline
11. Means, T. K., Golenbock, D. T., and Fenton, M. J. (2000) Structure and function of Toll-like receptor proteins. *Life Sci.* **68,** 241–258 CrossRef Medline
12. Danhier, F., Ansorena, E., Silva, J. M., Coco, R., Le Breton, A., and Préat, V. (2012) PLGA-based nanoparticles: an overview of biomedical applications. *J. Control Release* **161,** 505–522 CrossRef Medline
13. Steinhagen, F., Kinjo, T., Bode, C., and Klinman, D. M. (2011) TLR-based immune adjuvants. *Vaccine* **29,** 3341–3355 CrossRef Medline
14. Nempont, C., Cayet, D., Rumbo, M., Bompard, C., Villeret, V., and Sirard, J. C. (2008) Deletion of flagellin's hypervariable region abrogates antibody-mediated neutralization and systemic activation of TLR5-dependent immunity. *J. Immunol.* **181,** 2036–2043 CrossRef Medline
15. Casella, C. R., and Mitchell, T. C. (2008) Putting endotoxin to work for us: monophosphoryl lipid A as a safe and effective vaccine adjuvant. *Cell Mol. Life Sci.* **65,** 3231–3240 CrossRef Medline
16. Schneerson, R., Fattom, A., Szu, S. C., Bryla, D., Ulrich, J. T., Rudbach, J. A., Schiffman, G., and Robbins, J. B. (1991) Evaluation of monophosphoryl lipid A (MPL) as an adjuvant: enhancement of the serum antibody response in mice to polysaccharide-protein conjugates by concurrent injection with MPL. *J. Immunol.* **147,** 2136–2140 Medline
17. Shanmugam, A., Rajoria, S., George, A. L., Mittelman, A., Suriano, R., and Tiwari, R. K. (2012) Synthetic Toll like receptor-4 (TLR-4) agonist peptides as a novel class of adjuvants. *PLoS One* **7,** e30839 CrossRef Medline
18. Li, M., Jiang, Y., Gong, T., Zhang, Z., and Sun, X. (2016) Intranasal vaccination against HIV-1 with adenoviral vector-based nanocomplex using synthetic TLR-4 agonist peptide as adjuvant. *Mol. Pharm.* **13,** 885–894 CrossRef Medline
19. Arias, M. A., Van Roey, G. A., Tregoning, J. S., Moutaftsi, M., Coler, R. N., Windish, H. P., Reed, S. G., Carter, D., and Shattock, R. J. (2012) Glucopyranosyl lipid adjuvant (GLA), a synthetic TLR4 agonist, promotes potent systemic and mucosal responses to intranasal immunization with HIVgp140. *PLoS One* **7,** e41144 CrossRef Medline
20. Rudra, J. S., Tian, Y. F., Jung, J. P., and Collier, J. H. (2010) A self-assembling peptide acting as an immune adjuvant. *Proc. Natl. Acad. Sci. U.S.A.* **107,** 622–627 CrossRef Medline
21. Chiu, Y. C., Gammon, J. M., Andorko, J. I., Tostanoski, L. H., and Jewell, C. M. (2016) Assembly and immunological processing of polyelectrolyte multilayers composed of antigens and adjuvants. *ACS Appl. Mater. Interfaces* **8,** 18722–18731 CrossRef Medline
22. Park, B. S., Song, D. H., Kim, H. M., Choi, B. S., Lee, H., and Lee, J. O. (2009) The structural basis of lipopolysaccharide recognition by the TLR4-MD-2 complex. *Nature* **458,** 1191–1195 CrossRef Medline
23. Dunne, A., Mielke, L. A., Allen, A. C., Sutton, C. E., Higgs, R., Cunningham, C. C., Higgins, S. C., and Mills, K. H. (2015) A novel TLR2 agonist from *Bordetella pertussis* is a potent adjuvant that promotes protective immunity with an acellular pertussis vaccine. *Mucosal Immunol.* **8,** 607–617 CrossRef Medline
24. Shanmugam, A., Rajoria, S., George, A. L., Mittelman, A., Suriano, R., and Tiwari, R. K. (2012) Synthetic Toll like receptor-4 (TLR-4) agonist peptides as a novel class of adjuvants. *PLoS One* **7,** e30839 CrossRef Medline
25. Huang, Z. H., Shi, L., Ma, J. W., Sun, Z. Y., Cai, H., Chen, Y. X., Zhao, Y. F., and Li, Y. M. (2012) A totally synthetic, self-assembling, adjuvant-free MUC1 glycopeptide vaccine for cancer therapy. *J. Am. Chem. Soc.* **134,** 8730–8733 CrossRef Medline
26. Kushwaha, S., Singh, P. K., Gupta, J., Soni, V. K., and Misra-Bhattacharya, S. (2012) Recombinant trehalose-6-phosphate phosphatase of *Brugia malayi* cross-reacts with human *Wuchereria bancrofti* immune sera and engenders a robust protective outcome in mice. *Microbes Infect.* **14,** 1330–1339 CrossRef Medline
27. Tian, J., Wu, N., Guo, J., and Fan, Y. (2009) Prediction of amyloid fibril-forming segments based on a support vector machine. *BMC Bioinformatics* **10,** Suppl. 1, S45 CrossRef Medline
28. Bakou, M., Hille, K., Kracklauer, M., Spanopoulou, A., Frost, C. V., Malideli, E., Yan, L. M., Caporale, A., Zacharias, M., and Kapurniotu, A. (2017) Key aromatic/hydrophobic amino acids controlling a cross-amyloid peptide interaction *versus* amyloid self-assembly. *J. Biol. Chem.* **292,** 14587–14602 CrossRef Medline
29. Bortolini, C., Liu, L., Gronewold, T. M., Wang, C., Besenbacher, F., and Dong, M. (2014) The position of hydrophobic residues tunes peptide self-assembly. *Soft Matter* **10,** 5656–5661 CrossRef Medline
30. Sarroukh, R., Goormaghtigh, E., Ruysschaert, J. M., and Raussens, V. (2013) ATR-FTIR: a "rejuvenated" tool to investigate amyloid proteins. *Biochim. Biophys. Acta* **1828,** 2328–2338 CrossRef Medline
31. Othoro, C., Johnston, D., Lee, R., Soverow, J., Bystryn, J. C., and Nardin, E. (2009) Enhanced immunogenicity of *Plasmodium falciparum* peptide vaccines using a topical adjuvant containing a potent synthetic Toll-like receptor 7 agonist, imiquimod. *Infect. Immun.* **77,** 739–748 CrossRef Medline
32. Miconnet, I., Coste, I., Beermann, F., Haeuw, J. F., Cerottini, J. C., Bonnefoy, J. Y., Romero, P., and Renno, T. (2001) Cancer vaccine design: a novel bacterial adjuvant for peptide-specific CTL induction. *J. Immunol.* **166,** 4612–4619 CrossRef Medline
33. BenMohamed, L., Gras-Masse, H., Tartar, A., Daubersies, P., Brahimi, K., Bossus, M., Thomas, A., and Druilhe, P. (1997) Lipopeptide immunization without adjuvant induces potent and long-lasting B, T helper, and cyto-

toxic T lymphocyte responses against a malaria liver stage antigen in mice and chimpanzees. *Eur. J. Immunol.* **27,** 1242–1253 CrossRef Medline
34. Kushwaha, S., Singh, P. K., Rana, A. K., and Misra-Bhattacharya, S. (2013) Immunization of *Mastomys coucha* with *Brugia malayi* recombinant trehalose-6-phosphate phosphatase results in significant protection against homologous challenge infection. *PLoS One* **8,** e72585 CrossRef Medline
35. Dubois Cauwelaert, N., Desbien, A. L., Hudson, T. E., Pine, S. O., Reed, S. G., Coler, R. N., and Orr, M. T. (2016) The TLR4 agonist vaccine adjuvant, GLA-SE, requires canonical and atypical mechanisms of action for TH1 induction. *PLoS One* **11,** e0146372 CrossRef Medline
36. O'Garra, A., and Arai, N. (2000) The molecular basis of T helper 1 and T helper 2 cell differentiation. *Trends Cell Biol.* **10,** 542–550 CrossRef Medline
37. Alving, C. R., Peachman, K. K., Rao, M., and Reed, S. G. (2012) Adjuvants for human vaccines. *Curr. Opin. Immunol.* **24,** 310–315 CrossRef Medline
38. Coffman, R. L., Sher, A., and Seder, R. A. (2010) Vaccine adjuvants: putting innate immunity to work. *Immunity* **33,** 492–503 CrossRef Medline
39. De Souza Rebouças, J., Esparza, I., Ferrer, M., Sanz, M. L., Irache, J. M., and Gamazo, C. (2012) Nanoparticulate adjuvants and delivery systems for allergen immunotherapy. *J. Biomed. Biotechnol.* **2012,** 474605 Medline
40. Zhang, L., Hu, C., Yang, W., Liu, X., and Wu, Y. (2016) Chemical synthesis, versatile structures and functions of tailorable adjuvants for optimizing oral vaccination. *ACS Appl. Mater. Interfaces* **8,** 34933–34950 CrossRef Medline
41. Reed, S. G., Orr, M. T., and Fox, C. B. (2013) Key roles of adjuvants in modern vaccines. *Nat. Med.* **19,** 1597–1608 CrossRef Medline
42. Ireton, G. C., and Reed, S. G. (2013) Adjuvants containing natural and synthetic Toll-like receptor 4 ligands. *Expert Rev. Vaccines* **12,** 793–807 CrossRef Medline
43. Moyle, P. M., and Toth, I. (2013) Modern subunit vaccines: development, components, and research opportunities. *ChemMedChem* **8,** 360–376 CrossRef Medline
44. Rudra, J. S., Sun, T., Bird, K. C., Daniels, M. D., Gasiorowski, J. Z., Chong, A. S., and Collier, J. H. (2012) Modulating adaptive immune responses to peptide self-assemblies. *ACS Nano* **6,** 1557–1564 CrossRef Medline
45. Rudra, J. S., Mishra, S., Chong, A. S., Mitchell, R. A., Nardin, E. H., Nussenzweig, V., and Collier, J. H. (2012) Self-assembled peptide nanofibers raising durable antibody responses against a malaria epitope. *Biomaterials* **33,** 6476–6484 CrossRef Medline
46. Boato, F., Thomas, R. M., Ghasparian, A., Freund-Renard, A., Moehle, K., and Robinson, J. A. (2007) Synthetic virus-like particles from self-assembling coiled-coil lipopeptides and their use in antigen display to the immune system. *Angew. Chem. Int. Ed. Engl.* **46,** 9015–9018 CrossRef Medline
47. Schroeder, U., Graff, A., Buchmeier, S., Rigler, P., Silvan, U., Tropel, D., Jockusch, B. M., Aebi, U., Burkhard, P., and Schoenenberger, C. A. (2009) Peptide nanoparticles serve as a powerful platform for the immunogenic display of poorly antigenic actin determinants. *J. Mol. Biol.* **386,** 1368–1381 CrossRef Medline
48. Puffer, E. B., Pontrello, J. K., Hollenbeck, J. J., Kink, J. A., and Kiessling, L. L. (2007) Activating B cell signaling with defined multivalent ligands. *ACS Chem. Biol.* **2,** 252–262 CrossRef Medline
49. Aimanianda, V., Haensler, J., Lacroix-Desmazes, S., Kaveri, S. V., and Bayry, J. (2009) Novel cellular and molecular mechanisms of induction of immune responses by aluminum adjuvants. *Trends Pharmacol. Sci.* **30,** 287–295 CrossRef Medline
50. Marrack, P., McKee, A. S., and Munks, M. W. (2009) Towards an understanding of the adjuvant action of aluminium. *Nat. Rev. Immunol.* **9,** 287–293 CrossRef Medline
51. Stills, H. F., Jr. (2005) Adjuvants and antibody production: dispelling the myths associated with Freund's complete and other adjuvants. *ILAR J.* **46,** 280–293 CrossRef Medline
52. Kurihara, Y., and Furue, M. Interferon-γ enhances phorbol myristate acetate-induced cell attachment and tumor necrosis factor production via the NF-κB pathway in THP-1 human monocytic cells. *Mol. Med. Rep.* **7,** 1739–1744
53. Chen, R., Li, L., and Weng, Z. (2003) ZDOCK: An initial-stage protein-docking algorithm. *Proteins* **52,** 80–87 CrossRef Medline
54. Pettersen, E. F., Goddard, T. D., Huang, C. C., Couch, G. S., Greenblatt, D. M., Meng, E. C., and Ferrin, T. E. (2004) UCSF Chimera—a visualization system for exploratory research and analysis. *J. Comput. Chem.* **25,** 1605–1612 CrossRef Medline
55. Wallace, A. C., Laskowski, R. A., and Thornton, J. M. (1995) LIGPLOT: a program to generate schematic diagrams of protein-ligand interactions. *Protein Eng.* **8,** 127–134 CrossRef Medline
56. Scott, W. R. P., Hünenberger, P. H., Tironi, I. G., Mark, A. E., Billeter, S. R., Fennen, J., Torda, A. E., Huber, T., Krüger, P., and van Gunsteren, W. F. (1999) The GROMOS Biomolecular Simulation Program Package. *J. Phys. Chem. A* **103,** 3596–3607 CrossRef
57. Abraham, M. J., Murtola, T., Schulz, R., Páll, S., Smith, J. C., Hess, B., and Lindahl, E. (2015) GROMACS: high performance molecular simulations through multi-level parallelism from laptops to supercomputers. *SoftwareX* **1,** 19–25
58. Rallabhandi, P. (2010) Measuring TLR function in transfectants. *Curr. Protoc. Immunol.* Chapter 14, Unit 14.16 CrossRef Medline
59. Livak, K. J., and Schmittgen, T. D. (2001) Analysis of relative gene expression data using real-time quantitative PCR and the $2^{-\Delta\Delta CT}$ method. *Methods* **25,** 402–408 CrossRef Medline